small circle (Fig. 1) about the pole of relative plate motion (*11*). This finding suggests a left-stepping kink in the locus of elastic strain accumulation, roughly coincident with the location of the Big Bend and Transverse Ranges. Although the inferred JPL–Monument Peak relative motion is lessened by the most recent SLR findings, even a modest discrepancy of 1 cm/year results in similar conclusions. Such a distribution of elastic strain could be relevant to suggestions of local reorientation of the Pacific–North American plate slip direction in southern California (*19*). However, such "microplate" activity is not reflected directly in the present short-term measurements, which show a direction of motion parallel to the overall plate boundary.

The explanation of such an offset shear zone may depend on the nature of the forces that drive plate motions at the boundary. It has been suggested (*20*) that active convective downwelling in the mantle beneath the Transverse Ranges exerts tractions on the base of the lithosphere in this region. Alternatively, complex block motions within the transpressive restraining bend of the San Andreas (*14*) may elastically redistribute the strain. In this case, mantle convergence and downwelling beneath the Transverse Ranges kink assumes a more passive role.

Resolution of these questions must await more complete geodetic strain data and a more comprehensive understanding of the forces that drive short-term deformation of the crust and mantle. In particular, the rates of motion between OVRO, Monument Peak, and Quincy, upon which much of the above hypothesis rests, must be better determined before either the kinematics or the dynamics become well defined. It is expected that continuing measurements by VLBI (and other space-based geodetic techniques) incorporating more sites than those discussed here, coupled with conventional geodetic data, will further improve our understanding of strain accumulation and tectonic motion in western North America.

REFERENCES AND NOTES

1. J. M. Davidson and D. W. Trask, *IEEE Trans. Geosci. Remote Sensing* **GE-23**, 426 (1985).
2. I. I. Shapiro, in *Methods of Experimental Physics*, M. L. Meeks, Ed. (Academic Press, New York, 1976), p. 261; J. B. Thomas, *Tech. Rep. Jet Propul. Lab. Calif. Inst. Technol. 32-1526* (1972), vol. 7, p. 37; *ibid.*, vol. 8, p. 29; *ibid.* (1974), vol. 16, p. 47.
3. G. A. Lyzenga, K. S. Wallace, J. L. Fanselow, A. Raefsky, P. M. Groth, in preparation.
4. The derivation of baselines from raw VLBI data is itself a problem in model parameter estimation (*2*). Although the uncertainties directly attributable to measurement error are of principal importance, the magnitudes of systematic errors due to mismodeling of the measurement process may be significant. In this analysis, the uncertainties have been propagated through both the estimation processes involved in the baseline reduction process and the strain rate determination. In these analyses we have attempted to allow for the effect of unmodeled systematic effects, so that the quoted uncertainties are realistic.
5. J. C. Crowell, *Calif. Div. Mines Geol. Spec. Rep. 118* (1975), p. 7; in *Geotectonic Development of California*, G. E. Ernst, Ed. (Prentice-Hall, Englewood Cliffs, NJ, 1981), p. 583; T. H. Nilson, *Geol. Soc. Am. Bull.* **95**, 599 (1984).
6. K. E. Sieh and R. H. Jahns, *Geol. Soc. Am. Bull.* **95**, 883 (1984); E. A. Keller, M. S. Bonkowski, R. J. Korsh, R. J. Shlemon, *ibid.* **93**, 46 (1982).
7. J. C. Savage, *Annu. Rev. Earth Planet. Sci.* **11**, 11 (1983); ——, W. H. Prescott, M. Lisowski, N. E. King, *J. Geophys. Res.* **86**, 6991 (1981); W. Thatcher, *ibid.* **84**, 2351 (1979).
8. T. Atwater, *Geol. Soc. Am. Bull.* **81**, 3513 (1970).
9. R. L. Larson, H. W. Menard, S. M. Smith, *Science* **161**, 781 (1968); D. G. Moore and E. C. Buffington, *ibid.*, p. 1238; R. L. Larson, *Geol. Soc. Am. Bull.* **83**, 3345 (1972).
10. W. Hamilton, *Geol. Soc. Am. Bull.* **72**, 1307 (1961); J. Suppe, *ibid.* **81**, 3253 (1970).
11. J. B. Minster and T. H. Jordan, *J. Geophys. Res.* **83**, 5331 (1978).
12. ——, in *Tectonics and Sedimentation Along the California Margin*, J. K. Crouch and S. B. Bachman, Eds. (Pacific Section, Society of Economic Paleontologists and Mineralogists, Tulsa, OK, 1984), vol. 38, p. 1.
13. S. A. Graham and W. R. Dickinson, *Science* **199**, 179 (1978).
14. P. Bird and R. W. Rosenstock, *Geol. Soc. Am. Bull.* **95**, 946 (1984).
15. J. N. Louie, C. R. Allen, D. C. Johnson, P. C. Haase, S. N. Cohen, *Bull. Seismol. Soc. Am.* **75**, 811 (1985).
16. D. E. Smith, R. Kolenkiewicz, P. J. Dunn, M. H. Torrence, *Tectonophysics* **52**, 59 (1979); D. C. Christodoulidis *et al.*, *J. Geophys. Res.* **90**, 9249 (1985).
17. R. Kolenkiewicz *et al.*, *Eos* **66**, 246 (1985) (abstract); D. E. Smith *et al.*, *ibid.*, p. 848.
18. T. A. Clark and J. W. Ryan, *ibid.*, p. 246; P. M. Kroger, J. M. Davidson, S. A. Stephens, *ibid.*, p. 246.
19. R. Weldon and E. Humphreys, *Tectonics* **5**, 33 (1986).
20. E. Humphreys, R. W. Clayton, B. H. Hager, *Geophys. Res. Lett.* **11**, 625 (1984).
21. This research was carried out at the Jet Propulsion Laboratory, California Institute of Technology, under a contract with the National Aeronautics and Space Administration. We acknowledge the important contributions to this work by J. L. Fanselow and K. S. Wallace. We are grateful for helpful discussions with W. B. Banerdt, J. Davidson, T. Dixon, and E. Ivins. Results provided in advance of publication by D. Christodoulidis, P. Kroger, and M. A. Spieth were invaluable in the preparation of this report.

3 March 1986; accepted 6 May 1986

Colors of Objects in the Field of the Double Quasi-Stellar Object 1146+111B,C

J. ANTHONY TYSON AND CRAIG A. GULLIXSON

Color images of faint objects were used to test two hypotheses for the quasi-stellar object (QSO) pair 1146+111B,C: gravitational lens or massive string. Blue, red, and near-infrared CCD (charge-coupled device) images of the field of this QSO pair were examined for gravitational lens multiple-image candidates for all four QSO's in the field (B, C, D, and E). No third image of 1146+111B,C was found, down to 4 magnitudes fainter than BC. This result implies a compact lens mass distribution, if B and C are images of the same QSO. C appears to be redder than B in the wavelength region from 700 to 1100 nanometers. This raises the question of whether B and C are images of the same QSO. Three blue stellar objects of unusual color were found at plausible locations for multiple images of the other two QSO's in the field. A very red object was found at a plausible lens position. Under the hypothesis that B and C are lensed images, these color data severely restrict the possible lens models and imaged QSO multiplicities. One possibility is a compact lens mass of 4×10^{15} solar masses at a redshift of 0.8. Another is an S-shaped massive string. If the spectrum of any of the three anomalous blue objects were available, it would be possible to distinguish between these two models. However, it is difficult to fit the color and intensity data reported here to either simple string or black hole models. Overall, the simplest model consistent with all the data is the no-lens, no-string hypothesis: B and C probably are separate QSO's, but with some spectral similarities.

THE FIELD 1146+111 IS UNUSUAL in at least two respects. It contains an excess number of quasi-stellar objects (QSO's), and two of them have nearly identical redshifts. These two QSO's, B and C, are separated on the sky by 157 arc sec. Is it possible that light from a QSO has traveled on two gravitationally deflected paths around a massive foreground object, giving rise to the dual images B and C? Until now, seven such "gravitational lenses" with multiple QSO image separations of less than 8 arc sec have been discovered. These image separations are consistent with the idea that massive galaxies are the gravitational light deflectors. An image separation of 157 arc sec, if gravitational in origin, would imply a much more massive foreground object.

On the basis of spectra around 600 nm, Turner *et al.* (*1*) report a confirmation of Paczynski's (*2*) suggestion that the double QSO 1146+111B,C found by Hazard, Arp,

J. A. Tyson, AT&T Bell Laboratories, Murray Hill, NJ 07974.
C. A. Gullixson, Lowell Observatory, Flagstaff, AZ 86001.

and Morton (*3*) is two images of the same QSO at a redshift z of 1.012 ± 0.001. If B and C are images of the same QSO, either a compact dark mass or a massive string is a possible cause. This field was initially of interest because of the excess numbers of QSO's. This excess would be a natural by-product of certain gravitational lens scenarios, in which background QSO's are statistically brightened, and thus catalogs of QSO's would be biased toward gravitationally lensed QSO's. A massive string or lens responsible for BC can also produce multiple images of other QSO's of redshift greater than BC and nearby on the sky. Multicolor charge-coupled device (CCD) photometry of all objects within several arc minutes of BC can thus constrain the nature and position of the lensing object. We have obtained color images of this field, which allows a search for the predicted multiple images of other QSO's in this field. We used these color, intensity, and position data to examine the viability of simple lens or string models for the unusual double QSO B,C. We find that either model is unlikely.

We obtained multiple CCD images in three bands of the 1146+111 field on the night of 14 April 1986 UT with the AT&T Bell Laboratories CCD camera on the Lowell Observatory 1.1-m telescope. On-chip 2 by 2 pixel binning and a 2 : 1 focal reduction camera gave a field of 9.0×7.2 arc min with 2.6–arc sec per pixel, and an effective f ratio of $f/4$. Six 750-second exposures in J (380 to 530 nm), six 300-second exposures in R (600 to 720 nm), and six 300-second exposures in I (780 to 1100 nm), interspersed with exposures of five calibration standard stars, were obtained under photometric conditions. A new technique was used, allowing the telescope to be pushed to its quantum limit for imaging. The field was moved randomly 15 to 30 arc sec on the CCD between exposures; thus systematics and defects in individual exposures (bad pixels, sky fringing, and radiation events) were removed. Reconstructed median-filtered images were formed from the cleaned disregistered exposures: image processing, including adaptive median filtering (*4, 5*) and fractional pixel image restoration, yielded sky noise–limited images (field = 6×8 arc min) in J, R, and I.

Composite color images made from this field (red = I, green = R, blue = J) are shown in Figs. 1 and 2. The intensity window is wider in Fig. 1, so that the colors of brighter objects can be seen. Some interesting objects are labeled on a contour plot of the J image, shown in Fig. 3. We used the labeling convention of Arp and Hazard (*6*) for the four known QSO's in the field. The identical QSO pair BC is marked, along with QSO E ($z = 1.10$) and QSO D ($z = 2.12$) and other stellar objects brighter than 22.5 J magnitude. A foreground cluster of galaxies sufficient to produce gravitationally lensed QSO images B and C would be obvious in Fig. 2, where the faintest galaxies shown are J < 24 magnitude, or 3×10^{-7} photon per square centimeter per second per angstrom. No cluster is seen. Thus, either a gravitational lens or a massive string scenario must involve predominantly dark (no stars) matter.

We first outline the search strategy for the discovery of any other multiple QSO images, under the gravitational lens hypothesis. In general, a lens can lie anywhere between B and C and within a redshift range $0.2 < z < 0.9$. A lens can produce multiple images of background QSO's, on opposite sides of the apparent lens position. QSO's E and D are close to BC on the sky but behind BC (higher redshift). Thus E and D are likely candidates for multiple lensed QSO images. Wedge-shaped regions on the sky such as BEC (for QSO E) and CDE (for QSO D) must be searched for possible multiple images of the QSO's E and D. Given the observed angular separation of BC, it is probable that there would be at least one multiple image of E, to the north of the BC midpoint, especially if the apparent lens position is closer to B. The absence of a multiple image of D, to the west of BC, would set limits to the extent of the lens mass distribution. From Fig. 2 it can be seen that both D and E have two blue candidates. However, one of these blue objects, to the east of object 31, has the colors of a galaxy and is resolved in all three bands. Depending on the mass distribution of the lens, the secondary images of E and D may be faint. The near equality of the intensity of B and C may be an accident (as in the case of the lensed QSO 0937+561). There may also be a difference of up to 10^3 light-years in path length for such a pair of images, so that intrinsic QSO luminosity variations could appear as intensity differences and possibly color differences as well.

We searched these regions for stellar (unresolved) objects of unusual color in the catalog produced by the Faint Object Classification and Analysis System (FOCAS) automated photometry. FOCAS detected and measured the apparent brightness of all stars and galaxies in the field, a total of 327 objects to 24 J magnitude. Of 177 objects detected to 23 J magnitude, 112 matched the position of I objects, and 77 matched positions of R objects, in the common JI and JR areas. Most of these objects are galaxies. From the observed number counts of faint galaxies in our data, the catalogs are complete to $J < 23.2$, $R < 22.0$, and $I < 20.4$ magnitude. Thus, for blue objects, the matched catalog is complete to a color of $J - R > 0.5$, for $J < 22.5$ magnitude. Table 1 lists the names, $J - R$ and $R - I$ colors, J

Table 1. Colors of stellar objects in the 1146+111 field. Numbers in parentheses are the 1 σ statistical noise errors. Positions are relative to QSO B.

Name	J − R color	R − I color	J magnitude	Redshift	Right ascension (arc sec)	Declination (arc sec)
15	−0.15 (0.05)	0.41 (0.07)	21.02 (0.02)		43.4	135.5
C	0.37 (0.01)	0.31 (0.02)	18.55 (0.005)	1.012	−71.2	138.3
B	0.41 (0.01)	0.22 (0.02)	18.55 (0.006)	1.012	0	0
31	0.43 (0.04)	0.66 (0.07)	21.58 (0.03)		−152.2	76.3
D	0.52 (0.01)	0.13 (0.01)	17.85 (0.004)	2.12	104.4	27.9
E	0.56 (0.01)	0.19 (0.02)	18.30 (0.005)	1.10	−32.8	−47.5
27	0.70 (0.01)	0.37 (0.02)	18.75 (0.007)		−151.9	129.0
7	0.76 (0.01)	0.42 (0.01)	17.62 (0.003)		−0.4	204.1
8	0.81 (0.01)	0.36 (0.01)	17.78 (0.004)		2.8	258.8
17	0.83 (0.01)	0.30 (0.02)	18.01 (0.004)		91.4	46.5
5	0.88 (0.04)	0.44 (0.06)	21.71 (0.03)		−35.2	127.1
14	0.91 (0.03)	−0.21 (0.06)	21.27 (0.02)		−5.6	141.3
6	0.92 (0.01)	0.40 (0.01)	16.15 (0.003)		65.8	−79.1
18	1.03 (0.01)	0.54 (0.02)	17.83 (0.004)		77.4	63.9
2	1.10 (0.01)	0.51 (0.01)	18.04 (0.004)		−94.2	86.9
3	1.13 (0.01)	0.59 (0.01)	17.55 (0.003)		−122.8	106.3
10	1.39 (0.01)	0.74 (0.01)	18.12 (0.004)		−117.5	250.9
6.1	1.45 (0.01)	0.67 (0.01)	17.84 (0.004)		81.0	−109.3
9	1.45 (0.01)	0.72 (0.02)	19.53 (0.01)		−52.4	245.8
19	1.56 (0.02)	0.70 (0.03)	20.52 (0.015)		−190.2	210.0
4	1.84 (0.03)	1.41 (0.04)	21.47 (0.02)		−90.5	130.4
1	1.91 (0.01)	1.11 (0.01)	19.28 (0.01)		−66.5	48.4
20	1.91 (0.01)	1.34 (0.02)	20.75 (0.015)		−214.9	203.7
32	2.07 (0.05)	2.61 (0.03)	22.33 (0.04)		−226.1	42.7
22	2.08 (0.03)	1.60 (0.02)	21.38 (0.02)		−223.9	−92.0
37	2.48 (0.04)	1.58 (0.03)	22.40 (0.035)		−103.0	189.7
29	2.69 (0.07)	2.92 (0.04)	23.71 (0.06)		−12.2	57.0

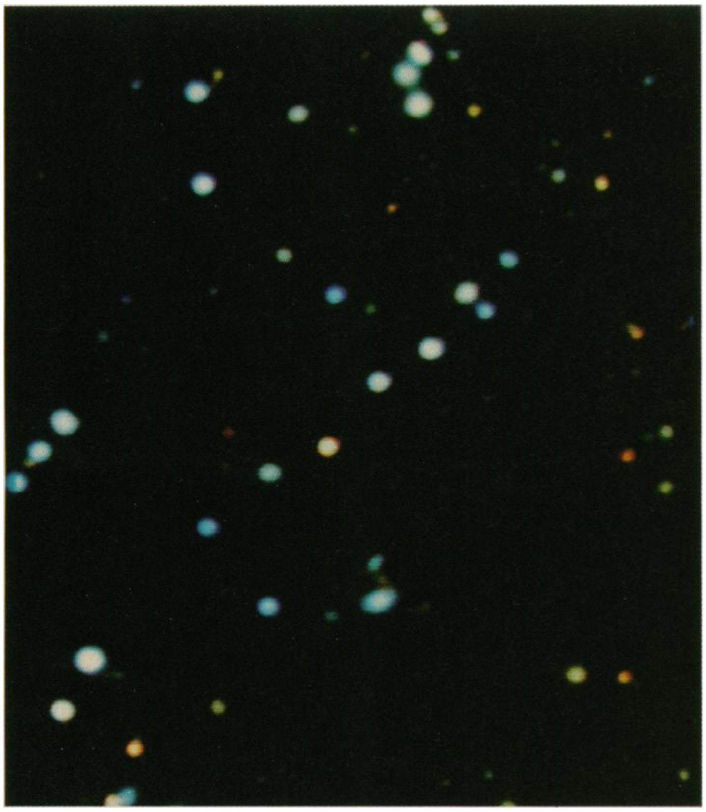

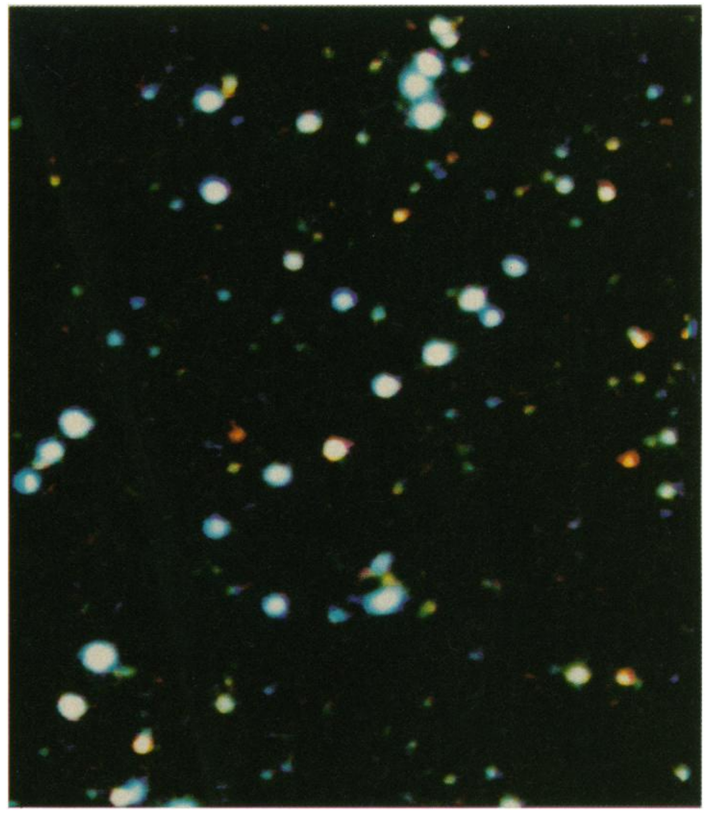

Fig. 1 (left). Color image of the 1146+111 field 6 × 8 arc min in size, made from 4500-second blue (J), 1800-second red (R), and 1800-second 1-μm (I) CCD exposures. In this composite color image, the colors have been shifted to be visible; red is $\log_{10}I$, green is $\log_{10}R$, and blue is $\log_{10}J$. The four known blue QSO's and three fainter BSO's, candidates for lens or string images of the QSO's, can be seen. See Fig. 3 for the naming conventions used for the interesting objects. North is up and east is to the left. Fig. 2 (right). The same composite color image data as in Fig. 1, but with an intensity window that displays fainter objects. The faintest objects with good signal-to-noise ratios have J < 23, R < 22, and I < 20 magnitude.

aperture magnitudes, redshifts (where known), and right ascension and declination offsets from QSO B, of the 26 stellar objects brighter than 22.5 J magnitude, and the red object 29. (The M dwarf 32 is probably contaminated with a background blue galaxy.) The position of star 6 is 11 46 14.27 +11 03 18 [1950]. QSO C is at 11 46 04.96 +11 06 56 [1950], and QSO B is at 11 46 09.80 +11 04 37 [1950]. The search for other fainter QSO's or other images of known QSO's in this field is best made by examining the colors of all stellar objects and comparing these to the colors of ordinary stars on the main sequence. A color-color plot of the colors (J − R, R − I) of these stellar objects relative to the main sequence in the JRI system is shown in Fig. 4. Below we discuss the stellar objects with interesting colors and positions, and test the hypotheses of gravitational lens or massive string.

From Table 1, C appears to be slightly (2 σ) redder than B in the wavelength region from 0.7 to 1 μm. Although this could be due to absorption by an intervening galaxy, spectra of B and C in this wavelength region are warranted. The color of B from 0.4 to 0.7 μm also appears to be different from that of C. It is possible that B and C are separate QSO's with very similar spectra in the wavelength range investigated by Turner *et al.* (*1*). The number and relative brightness of multiple QSO images is a strong constraint on the lens mass distribution. Three images, within 3 magnitudes, are expected for most smooth spherically symmetric galaxy profiles, whereas two images are expected for a more compact black hole. Table 1 indicates that no third image of BC, within 5 σ of the same color, is found down to 4 magnitudes fainter than B and C. This implies that any lens responsible for B and C is at least as compact as an isothermal (density proportional to the inverse square of the radius) distribution. Thus, multiple images of E and possibly D would be likely. There are no stellar objects detected with colors similar to the four known QSO's in the field, down to 4.6 magnitudes fainter than D, 4.2 magnitudes fainter than E, and 4 magnitudes fainter than B and C. Thus it will be difficult to explain the identical nature of B and C (if true) on the basis of either simple lens or string models. Although the density of blue stellar objects (BSO's), aside from the known QSO's, is no higher than in several control fields, the BSO density is higher northeast of BC than in any other direction.

The peculiar-colored BSO's 14 and 15 are near the expected positions for multiple images of QSO E, for a lens centered nearer to B than to C. Spectroscopy of these 21 magnitude objects should reveal QSO spectra with the redshift of E, if this hypothesis is correct. Figure 4 suggests that object 14 has excess emission in our R band, consistent with the MgII emission at 586 nm in the spectrum of QSO E. The colors of object 15 suggest a QSO or an HII region. The flux ratio between QSO E and object 14 at 500 nm is a factor of 15. This is consistent with an isothermal or slightly smoother lens mass distribution. The case for another image of QSO D is less compelling but should also be checked with spectroscopy: BSO 31, although it appears to have colors of a $z = 1$ spiral galaxy, sits in a likely area for an image of QSO D. It may be that these BSO's of unusual color, like 14, 15, and 31, are lensed images of other fainter QSO's in the field. There is an additional coincidence in this field: stellar objects 2 and 3, separated by 34 arc sec, have nearly the same colors.

As an alternative to a massive gravitational lens, a massive string (*7*) with a density of 4×10^{23} g/cm could in principle give the observed separation of BC (*8*). Because B and C have nearly the same flux, the simplest string would lie nearly orthogonal to BC and would also probably bisect BC (in order

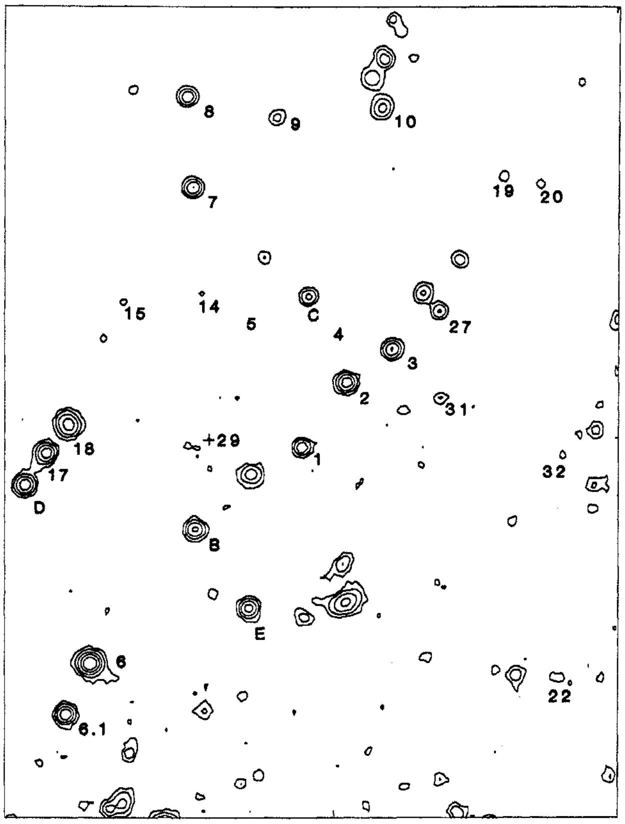

Fig. 3. A logarithmic flux contour plot of the 4500-second J image, 6 × 8 arc min in size. North is up and east is to the left. The nearly identical QSO pair BC at redshift $z = 1.012$ is marked. QSO E at $z = 1.10$ and QSO D at $z = 2.12$ are indicated. Stellar objects from Table 1 are numbered. Note the very red object (29) in Figs. 1 and 2. It is difficult to draw any simple projected massive string, consistent with the positions of the observed blue stellar objects, with nonstellar colors.

to guarantee equal travel times for the two rays) in the general case where the parent QSO varies in luminosity on 10- to 1000-year time scales. This would almost certainly lead to second images of both D and E. That is, if a massive string is responsible for the double QSO BC, then any other background QSO's would in general also have multiple images, if their ray paths pass close enough to the string. In order for object 14 to be the image of D, and object 31 to be the image of E, the string would have to be S-shaped (two adjustable parameters) but would not bisect D-14 or E-31, so that the second images of D and E are fainter. This is possible because differences in path length occur for nonequal subimage-string angles: for a string between $z = 0.2$ and 0.6, path length differences of 240 to 3900 light-years for D and 450 to 4500 light-years for E would occur (*9*). Thus, intrinsic source variations can give rise to some brightness (and probably slight spectral) differences between the QSO images. Virtually nothing is known about intrinsic QSO luminosity variations on these long time scales. However, the fact that the candidate secondary images of QSO's D and E, generated by this hypothetical string, are over 4 magnitudes fainter than D and E, and have dissimilar colors, makes the string models unlikely and rather contrived. A critical test will be the examination of the spectra of objects 14, 15, and 31. If object 14 is a QSO at $z = 2.12$ and object 31 is a QSO at $z = 1.10$, then the massive string hypothesis would hold. We now discuss the possibility of a massive lens.

Without spectra of these objects, it is premature to discuss any lens model at length. Nevertheless, from our color data, certain image multiplicity–lens model possibilities can now be ruled out. Let us consider spherical isothermal or black hole lens mass distributions. For these gravitational effects on light rays, isothermal distributions are most naturally expressed in terms of their velocity dispersion, while black holes are expressed in terms of their mass. If objects 14 or 15, or both, are images of E, this 192–arc sec separation together with the BC separation yields a solution for a single isothermal lens with a velocity dispersion of 3600 km/sec at $z = 0.7$. According to this model, object 31 is not a lensed image of QSO D. A single black hole, although it provides little amplification, is consistent with all the above suggested images and would have a mass of 4.5×10^{15} solar masses (in units where the Hubble constant H is 100 km per second per 10^6 parsecs) at $z = 0.8$. However, a massive black hole would not create a pair of highly magnified images of a background QSO and thus would not provide a natural explanation for BC and the QSO excess in this field. In either case, any such lens is apparently accompanied by very little luminous matter. The area density of galaxies brighter than 23 J magnitude is nearly equal to that in several control fields. Roughly 1000 such galaxies would be expected in the BC region, if the gravitational lens mass is in the form of protons and neutrons (baryonic). Although the density of $J < 20$ magnitude galaxies is five times the expected level based on control fields, there is no sign of the rich cluster appropriate to a velocity dispersion of 2000 to 3000 km/sec. Such a massive pile of baryonic matter would scatter microwave background photons. The null results of Stark *et al.* (*10*) are consistent (*11*) with this high mass-to-luminosity but low baryon fraction. They found no evidence for a change in the cosmic microwave background radiation in the direction of 1146+111B,C. Of course, this result is also consistent with the hypothesis that B and C are separate QSO's, and that there is no lens or string responsible for this unusual arrangement.

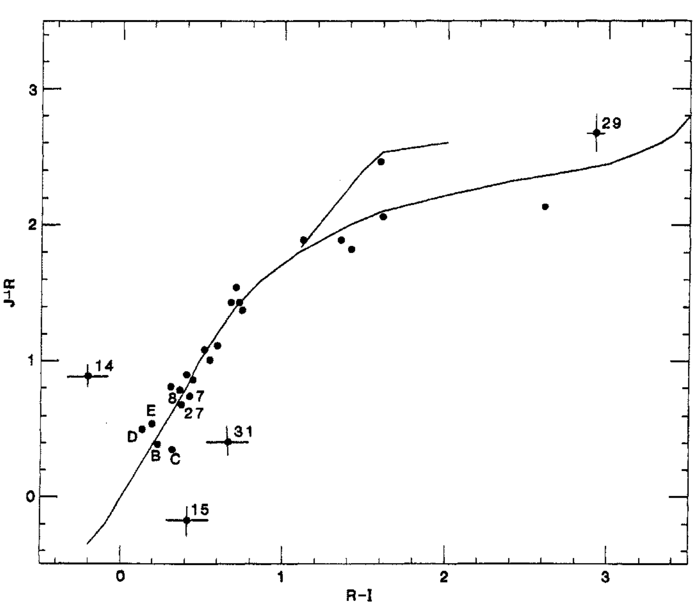

Fig. 4. Color-color plot J − R versus R − I of the stellar objects brighter than J = 22.5 magnitude. The main sequence in this JRI system, determined from a separate stellar survey (*14*), is shown as a solid curve. Note the three blue objects of nonstellar colors (14, 15, and 31) and the red object (29). Error bars of the interesting faint objects are ±2 σ.

It may be no accident that the only infrared-excess object in the field, object 29, with $J - R = 2.69$, $R - I = 2.92$, and $I = 18.10$ magnitude, is close to a probable lens position. It is clearly seen in Figs. 1 and 2. Its colors are less consistent with an elliptical galaxy ($z = 0.8$ to 1) than with an M6 (16th absolute magnitude at 550 nm) red dwarf star, and its R image looks stellar. The presence of an 18th I magnitude dwarf star in this field of 6×8 arc min is moderately unlikely: over the range of stellar luminosity functions compatible with current survey data, we expect between 0.01 and 0.1 M6 or later star in this field brighter than 18th I magnitude. If it were an Infrared Astronomical Satellite (IRAS) galaxy like Arp 220 (10^{12} solar luminosities), at $z = 0.8$ to 1, with a mass-to-luminosity ratio of 100, it would escape detection in the IRAS catalog. No IRAS source is seen at that location. Spectroscopic studies of object 29 in the red, to examine the possibility that it is an accidental foreground M dwarf star, are warranted. Recent JHK infrared photometry (*12*) confirms it as an M dwarf.

Given that 1146+111B,C are dual images of the same QSO, we reach the following conclusions about the gravitational light-deflecting object. Overall, our data on the 1146+111 field are less consistent with simple string and single massive black hole models than with the idea of an isothermal or slightly smoother mass distribution in a foreground lensing object. It is possible that this dark matter is lumpy, that is, not spherically symmetric as assumed in the lens models, giving rise to multiple images, some demagnified, of many background QSO's in the field. This idea would be supported by the discovery that objects 14, 15, and 31 are QSO's but not images of BC, D, or E.

However, the possibility must be considered that B and C are spectrally similar but physically separate QSO's. By far the simplest explanation for our data would be the seemingly unlikely possibility that B and C are separate QSO's. Recent blue spectra of B and C (*13*) show differing CIII line emission in the two QSO images. Although this difference might be attributable to rather contrived changes in the parent QSO emission over perhaps hundreds of years, together with corresponding differences in the travel time of light in the lens or string models, it will be difficult to make such models fit all the present color, intensity, position, and spectroscopic data.

REFERENCES AND NOTES

1. E. L. Turner *et al.*, *Nature (London)* **321**, 142 (1986).
2. B. Paczynski, *ibid.* **319**, 567 (1986).
3. C. Hazard, H. Arp, D. C. Morton, *ibid.* **282**, 271 (1979).
4. P. Seitzer, J. A. Tyson, H. Butcher, in preparation.
5. J. A. Tyson, P. Seitzer, R. J. Weymann, C. Foltz, *Astron. J.* **91**, 1274 (1986).
6. H. Arp and C. Hazard, *Astrophys. J.* **240**, 726 (1980).
7. A. Vilenkin, *ibid.* **282**, L51 (1984).
8. J. R. Gott, *ibid.* **288**, 422 (1985).
9. ———, *Nature (London)* **321**, 420 (1986).
10. A. A. Stark, M. Dragovan, R. W. Wilson, J. R. Gott, *ibid.*, in press.
11. J. P. Ostriker and E. T. Vishniac, *ibid.*, in press.
12. H. Thronson, *Int. Astron. Union Circ. 4227* (1986).
13. J. P. Huchra, *Nature (London)*, in press.
14. P. C. Boeshaar and J. A. Tyson, *Astrophys. J.* **90**, 817 (1985).

15. We are indebted to N. Hartsough for his expert software support, under pressure, and to G. Grasdalen and S. J. Bus who helped with the astrometry. We thank E. Turner for supplying a preprint, and R. Gott, J. Huchra, E. Turner, J. Bally, and P. Boeshaar for helpful discussions.

15 May 1986; accepted 20 June 1986

Females' Choice of "Good Genotypes" as Mates Is Promoted by an Insect Mating System

WARD B. WATT,* PATRICK A. CARTER, KATHLEEN DONOHUE

Can animal mating systems result in the choice of mates carrying genotypes that are otherwise favored by natural selection? This question is addressed by studying, in natural populations of *Colias* butterflies, how the phosphoglucose isomerase (PGI) enzyme genotype of males mating *Colias* females varies with degree of female mate discrimination. Certain PGI genotypes (as predicted from their biochemical properties) have been found previously to have an advantage in diverse fitness-related properties: flight capacity, survivorship, and overall mating success. It is shown here that males of these same genotypes have even greater advantage in remating older, more discriminating females than they do in mating previously unmated, less discriminating females. Assortative mating is not found and thus cannot explain this effect. The mating system of these insects does, at least in this case, result in active female choice of generally favorable male genotypes as mates.

A QUESTION OF INTEREST IN EVOLUTIONARY biology is whether sexual selection can drive the evolution of generally adaptive characteristics or only the evolution of those features directly useful in securing mates (*1–5*). Do mating systems evolve so that animals choose mates carrying the most fit genotypes, whose offspring are likely to be generally fit? Does mate selection by one sex mainly concern display or recognition characteristics of the other sex? Or, is evolutionary reality a mixture of these extremes? Selection for male display characteristics, whether mediated by male-male competition, female choice, or a mixture of these, is well documented (*5*). Mate selection for generally adaptive phenotypes has been found in several systems (*2, 3, 6*), but evidence that generally adaptive genotypes are thus favored is rare (for example, *3, 4, 7*). This rarity may stem from the fact that the causes of fitness differences, or of differences in fitness components, have seldom been traced to alternative genotypes of any specific loci (*8*).

Pierid butterflies, especially the genus *Colias* (the "Sulfurs"), are now widely used as a model system for study of evolutionary processes, including sexual selection (*9–13*). *Colias*' mating is governed by a males-find-and-court, females-choose system (*11–13*). Courtship signals used are visual patterns, short-range pheromones, and male courtship flight and "wing-flicking" (*12–15*). Discrimination in acceptance or rejection of potential mates, on the basis of these signals, by an unmated female increases dramatically during the first hour of adult life (*11*), and in the laboratory (*16*) continues to do so for 24 hours. This choice does not depend on male-male competition but is exercised with respect to individual males. Once mated, females become, for several days, refractory to further courtship. In *Colias*' relative *Pieris*, this results from distension of the female bursa copulatrix, caused by the spermatophore that the male deposits there during copulation; hormonal cues may also be involved (*17*). The spermatophore carries both sperm and nutrients that may be used by the female (*18, 19*). Resistance to remating later declines, and females remate up to three times in the wild (*14*). While a male may need as little as 5 seconds to court a young unmated female successfully (*11*), a male's persistence in courtship flight does on average increase his chance of mating an unmated female in the field (*20*). Male persistence is crucial to successful remating

Rocky Mountain Biological Laboratory, Crested Butte, CO 81224 and Department of Biological Sciences, Stanford University, Stanford, CA 94305.

*To whom correspondence should be directed (at the Stanford address).